UNIVERSITY OF CALIFORNIA, SAN DIEGO

Conservation of plant defense responses observed in microalgae-fungal pathogen interactions

A thesis submitted in partial satisfaction of
the requirements for the degree Master of Science

in

Biology

by

Fiona Margaret Nohilly

Committee in charge:

Professor Steven P. Briggs, Chair
Professor Maarten J. Chrispeels
Professor Stephen P. Mayfield

2013

The thesis of Fiona Margaret Nohilly is approved, and it is acceptable in quality and form for publication on microfilm and electronically:

_____

_____

_____

Chair

University of California, San Diego

2013

DEDICATION

I dedicate this thesis to Barbara McClintock for her inspiration and remarkable impact on the world of science.

TABLE OF CONTENTS

LIST OF ABBREVIATIONS

AAA: aromatic amino acid

ABA: abscisic acid

AGP: arabinogalactin protein

BTH: Benzothiadiazole

CAD: cinnamyl alcohol dehydrogenase

Chytrid: Chytridiomycota

CS: chorismate synthase

DHAP: 3-deoxy-D-arbino-heptulosonate 7-phosphate

DMSO: dimethyl sulfoxide

EPSP: 5-enolpyruvylshikimate-3-phosphate

ET: ethylene

ETI: Effector-triggered immunity

HEPES: 4-(2-hydroxyethyl)-1-piperazineethanesulfonic acid

HR: hypersensitive response

iTRAQ: isobaric tag for relative and absolute quantitation

ITS: Internal transcriber spacer

PCR: polymerase chain reaction

qPCR: quantitative (real-time) polymerase chain reaction

JA: jasmonic acid

LC: liquid chromatography

LOX: lipoxygenase

LRR: leucine rich repeat

MASM (D): modified artificial salt medium

MeJA: methyl jasmonate

MeSA: methyl salicylate

MS: mass spectrometry

NB-LRR: nucleotide-binding leucine rich repeat

NT: no treatment

OD: optical density

PAMP: pathogen-associated molecular pattern

PCD: programmed cell death

PI: post infection

PR: pathogenesis-related

PTI: PAMP-triggered immunity

R protein: resistance protein

RFU: relative fluorescence units

ROS: reactive oxygen species

RP: reverse phase

RPM: rotations per minute

S. dimorphus: Scenedesmus dimorphus

SA: salicylic acid

SCX: strong cation exchange

SDS: sodium dodecyl sulfate

SK: shikimate kinase

LIST OF FIGURES

LIST OF TABLES

ACKNOWLEDGMENTS

Steve, for being an incredible advisor and teacher. Thank you for the opportunity to work on this project and unwavering support throughout this project. The time I have spent in the lab has not only taught me valuable basic research skills and system biology tools but it has helped me discover my passion for research and inspired me to pursue a career in scientific research.

Rob, for being an exceptional mentor. From the beginning of my work on this project you have always been available to help me learn the skills I needed including everything from lab techniques to writing to time management. Rob's help and contributions to this project have been crucial to its success.

Sophie, for being an outstanding lab partner and mentor. You were extremely influential in the writing of this thesis. Your contribution to this project in this past year has allowed it to proceed further than I ever imagined and I have learned so much more than I ever anticipated. You have helped me in so many ways through the past year and I am very grateful for being able to work with you on this project.

Zhouxin, for your work on protein extraction and mass spectrometry analysis. Thank you for helping me learn more about mass spectrometry and your guidance on many aspects of this project.

Kyle, for your help with techniques, troubleshooting, interpreting results, and experimental design. Thank you for your input, assistance, and guidance on many aspects of this project. And for providing a fun working environment.

Sal, for your help with chytrid samples and showing me how to appreciate the wonderful world of microscopy. Thank you for being an inspirational colleague.

ABSTRACT OF THE THESIS

Conservation of plant defense responses observed in microalgae-fungal pathogen interactions

by

Fiona M. Nohilly

Master of Science in Biology

University of California, San Diego, 2013

Professor Steven P. Briggs, Chair

Outdoor ponds are the most practical means to cultivate algae for biofuel production. *S. dimorphus*, a green microalga with potential use as a biofuel crop, grown in ponds is susceptible to infection and disease caused by primitive chytrid-like fungi. Infection can kill virtually all of the algal cells in a pond within days. As a first step toward the development of resistant strains, we advanced our molecular understanding of algae and chytrid-like fungi interactions by observing infection-induced changes in the levels of proteins of *S. dimorphus*. Peptide mass spectrometry revealed ~2,500 proteins

change in abundance in *S. dimorphus* after FD61 (chytrid-like fungi) infection. We observed several proteins to be homologous to proteins involved in plant defense including proteins known to be precursors of plant defense hormones Salicylic Acid (SA) and Jasmonic Acid (JA). SA mediates defense against biotrophic pathogens while JA mediates defense against necrotrophic pathogens. BTH (SA analog) treatment of *S. dimorphus* delays FD01 infection and meJA treatment of *S. dimorphus* accelerates FD61 infection. BTH and meJA treatment at high concentration suppresses *S. dimorphus* growth (non-infected). We hypothesize that if SA and JA pathways exist in algae, a mutant less sensitive to JA will be less susceptible to chytrid infection and a mutant less sensitive to SA will be more susceptible to chytrid infection. To further test this hypothesis we will perform a library screen to find such a mutant and test candidates for susceptibility to chytrid infection.

INTRODUCTION

Algae biofuel as an alternative to fossil fuels

As the global population rises we continue to increase our use of energy. The majority of our energy comes from burning fossil fuels that emit harmful green house gases, such as CO2, and contribute to global warming (Stephens et al., 2010). Alternative energy resources must be established and utilized to meet future energy consumption demands. Algae biofuel which uses sunlight and CO_2 to grow can produce oil which can be refined in existing infrastructure, is a fungible fuel showing promise as an renewable alternative to fossil fuel (Chisti, 2007; Radakovits et al., 2010)

The sun harnesses over 85,000 terawatts of energy per year, which is over 5,000 times the amount of energy the world uses each year (Jones and Mayfield, 2012). Plants and algae are able to capture this sunlight energy and convert it to chemical energy through photosynthesis. Algae, like other terrestrial plants, utilize the process of photosynthesis to convert sunlight, carbon dioxide, and water to chemical energy that is stored as lipids, proteins, and carbohydrates (Chisti, 2007)

Algae use the energy from photosynthesis to accumulate storage lipids (e.g. triacylglycerides (TAGs)) (Guschina and Harwood, 2006), which can be converted into gasoline or jet fuel though distillation and cracking (Luo et al., 2010). It has been shown that many species of algae can produce lipids up to 50-60% of their dry biomass weight (Jones and Mayfield, 2012). We can harvest the oil from algae to produce the crude oil, which can be refined using the infrastructure of our current oil refineries.

Algae can be grown on marginal land using brackish or non-potable water (Borowitzka and Moheimani, 2010; Venteris et al., 2013) so it is not competitive with

production of food. Additionally algae grow much faster than terrestrial plants, and certain strains have been shown to be able to grow in a variety of harsh conditions including high temperature and salinity. In additional to being a potential energy source, recently it has been shown that the green alga *C. reinhardtii* has the ability to produce recombinant proteins, for example ability or antigen domains of vaccine candidates that can be used in therapeutic drug development (Tran et al., 2013).

Microalga *Scenedesmus dimorphus* is a potential biofuel crop

An alga with significant potential to be grown for the production of biofuels is *Scenedesmus*; a small, non-motile green algae from class *Chlorophyceae*. *Scenedesmus* sp. is high in lipid content and biomass productivity, critical components of biofuels, in comparison with other green algal strains (Rodolfi et al., 2009; Jena et al., 2012; Prabakaran and Ravindran, 2012). *Scenedesmus* sp. is able to tolerate a range of temperatures from 10-30C which makes it ideal for outdoor growth where temperatures can fluctuate thorough the day (Li et al., 2011). *Scenedesmus* sp. has also been shown to be capable of removing potentially hazardous materials, such as inorganic salts of nitrogen and phosphorus, from waste-water (Makarevi et al., 2011). Economic feasibility of algae growth on an industrial scale involves the use of large-scale cultivation in outdoor ponds. This set up is relatively low cost but involves high risk of contamination for pathogens from the surrounding environment (Georgianna and Mayfield, 2012). Until recently, algae have not been grown as a crop on a large scale and suitable cultivation systems and techniques are still being developed.

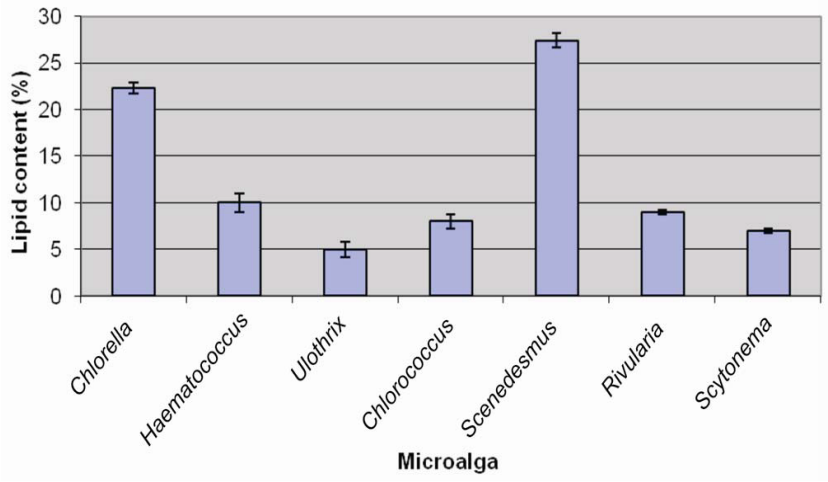

Figure 1: Lipid content of various strains of microalgae

Scenedesmus sp. accumulates 25-28% (of dry weight) lipid content and is high in lipid content compared other strains of microalgae (Prabakaran and Ravindran, 2012).

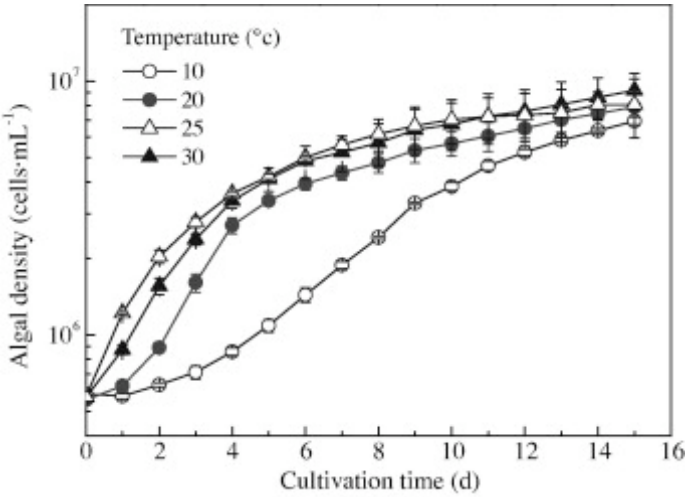

Figure 2: *Scenedesmus* sp. tolerates high temperatures

Scenedesmus can tolerate temperatures from 10-30C allowing it to be grown outside where temperatures can vary significantly throughout the day (Li et al., 2011)

Figure 3: Outdoor growth of *Scenedesmus dimorphus*

Outdoor growth of *Scenedesmus dimorphus* in raceway ponds at Sapphire Energy's Test Facility in Las Cruces, New Mexico. Left pond showing a contaminated, brown pond versus the right pond showing non-contaminated green pond.

Algae are susceptible to parasitic chytrid-like fungi

Green algae have been shown to be susceptible to parasitic fungi belonging to phyla Blastocladiomycota (Hoffman et al., 2008) and recently characterized Cryptomycota (Letcher et al., 2013). Our collaborators at Sapphire Energy have isolated three chytrid-like fungi from their ponds in New Mexico. "FD01" was recently characterized as *Amoeboaphelidium protococcarum* in the phyla Cryptomycota (Letcher et al., 2013). The two other parasitic fungi isolated are named "FD61" and "FD95" are also thought to be chytrid-like organisms. These fungi pose a significant challenge to cost effective growth of algae in outdoor ponds for the production of biofuels. Disease phenotypes include agglutination, loss of chlorophyll, and cell death. These fungi are related to Chytridiomycota or 'chytrids' which are characterized as a group of

microscopic fungi (Kendrick; Barr, 1980; Barr, 2001) that produce motile zoospores (Sparrow, 1960). These zoospores attach to the host cell wall, insert their hypha, and use the nutrients of the algae cell to reproduce, creating more zoospores, in a sporangia structure creating more zoospores. At that point the sporangia bursts and the zoospores are released; the cycle then repeats itself (Hoffman et al., 2008; Letcher, 2013).

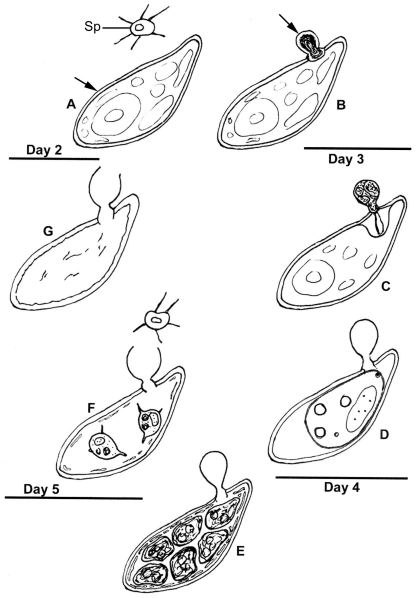

Figure 4: Life cycle schematic of *Amoepheledium protococcarum*

Day 1 and 2: Abundance of healthy algae cells. Day 3: Aplanospores attach to healthy algae cells, encyst on host through haustoria. Day 4: Contents of the host are degraded and spores reproduce inside algal host. Day 4: Aplanospores release from sporangia and are motile (Letcher et al., 2013).

Chytrids have been found in both marine and freshwater aquatic habitats and moist soils (Ibelings et al., 2004) and despite their need of water for zoospore reproduction, they heavily populate dry soil communities at high elevation (Freeman et al., 2009). Chytrids can function by feeding on debris, saprobes, or being dependent on the survival of the host, facultative or obligate parasites (Nichols et al., 1998; Margulis

and Chapman, 2009). Notably chytrid *Batrachochytrium dendrobatidis* is known for its involvement in the rapid decline of amphibians population (Piotrowski et al., 2004).

In order to protect the algae from invaders, like chytrids, it is necessary to have an understanding of mechanisms of infection and possible mechanisms of resistance to help create immunity. The knowledge of algae pathogen interactions and algal immunity is fairly limited in comparison to what has been discovered in plants. Research in the development of plant immunity has already elucidated many possible mechanisms of innate as well as evolved immunity in plants.

Green algae gave rise to higher plants, thus we hypothesize that *S. dimorphus* possess the evolutionary origins of the higher plant immune system. If this turns out to be true, then the extensive knowledge of plant immunity can be used to guide breeding and engineering efforts to develop disease-resistant algal strains.

Overview of Plant Defense Response

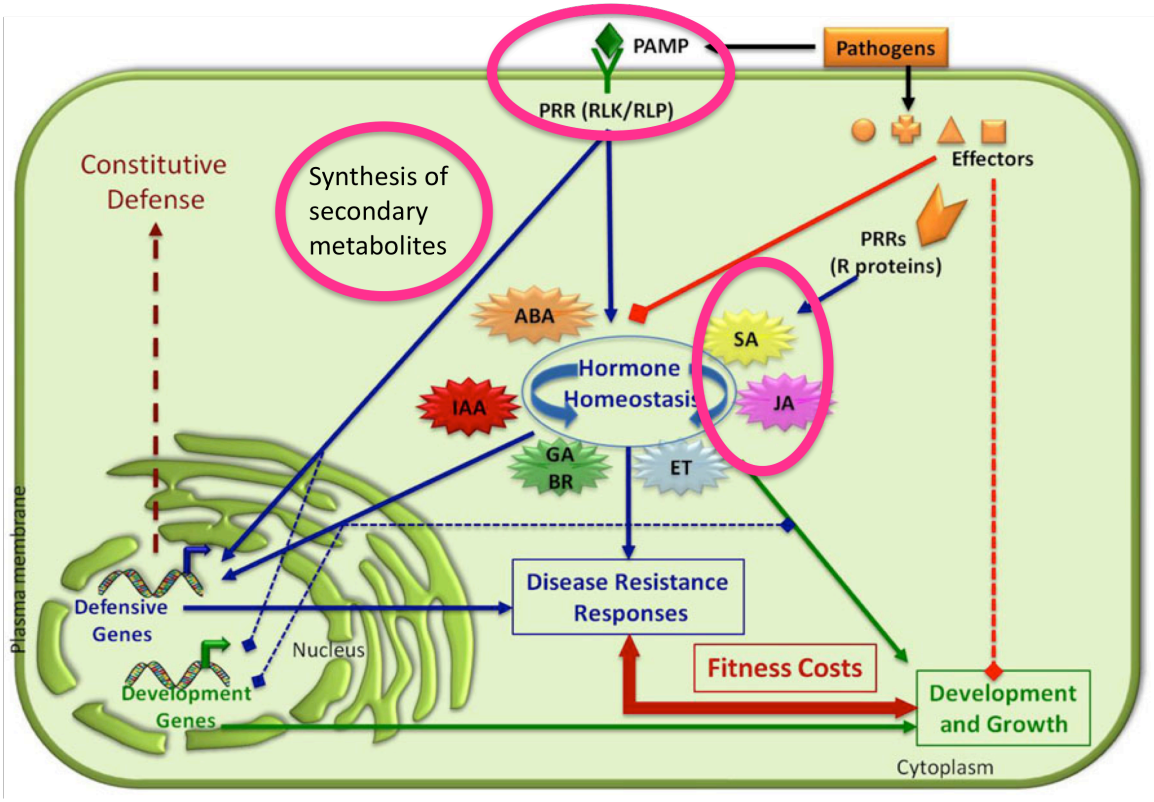

Figure 5: Overview of plant defense

Plants mediate defense by perception of pathogen via Pathogen associated molecule patterns (PAMPs) or effector molecules. Recognition of pathogens via PAMPs induces a disease resistance response mediated by hormones (such as SA and JA) and defensive genes. Effector molecules can also stimulate hormones and cause changes in development and growth. Plant defense is also mediated by other secondary metabolites (Denancé et al., 2013).

Plant resistance was first noticed through pathogen-associated molecular patterns (PAMPs), such as bacterial flagellin or fungal chitin, and caused PAMP-triggered Immunity (PTI). The pathogens have evolved to bypass this immune response by use of a type III secretion system to deliver effector proteins that target several key host proteins in the PTI mechanism. The creation of susceptibility in the host caused the host to invoke a second immune response, R proteins which recognize effectors secreted by the pathogen, restoring resistance again in the plant (Chisholm et al., 2006). We hypothesize

that algae may have a similar immune response to pathogen attack. We are interested in how these chytrid-like fungi are able to successfully parasitize *S. dimorphus* and if there are conserved PAMPs and/or effector molecules similar to what we have seen in plant pathogens. Chytrid fungi posses chitin (Gerphagnon et al., 2013) which could be recognized as a PAMP by the algae and possibly play a role in a PTI response in algae. This knowledge could deepen our understanding of how the algal host responds to infection and lead to the development of techniques of improving the algal host's ability to respond to infection by various pathogens. Moreover, with the exception of interactions between bacteria and phase, knowledge about the immune system in unicellular organisms is limited. Understanding the immune response of *S. dimorphus* would also give more insight into immunity in unicellular organisms.

Plant biotic stress hormones

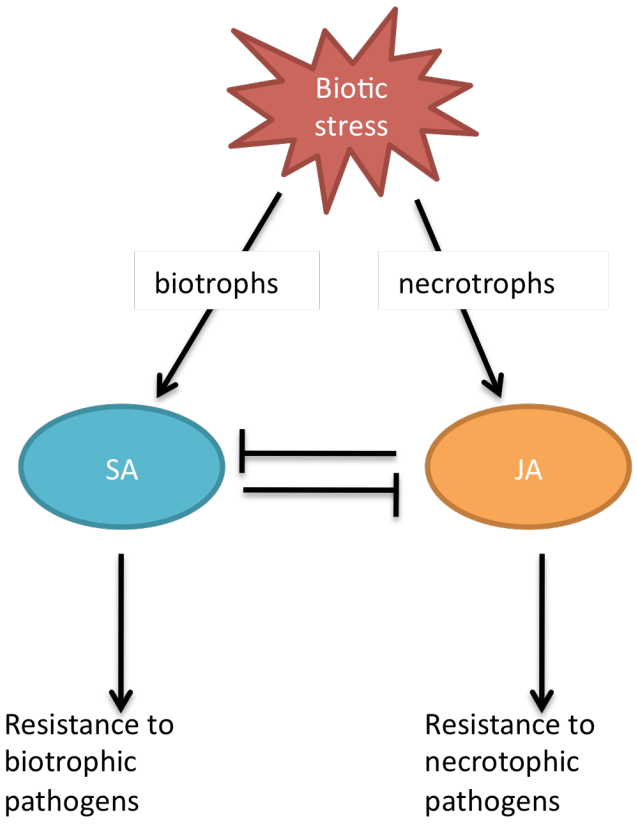

Figure 6: An overview of plant defense hormones

Schematic plant defense hormones and their cross talk. Recognition of biotrophic pathogens stimulates production of Salicylic Acid (SA) thereby induces resistance to biotrophic pathogens. Recognition of necrotrophic pathogens stimulates production of Jasmonic Acid (JA) thereby inducing resistance to necrotrophic pathogens. There is a mutual antagonistic relationship between defense against biotrophic pathogens mediated by SA and necrotrophic pathogens mediated by JA.

Plant receptors for pathogen-produced molecules activate biosynthesis of the stress hormones salicylic acid (SA) and Jasmonic acid (JA) triggers signals that induce defense against biotrophic pathogens and necrotrophic pathogens, respectively (Pieterse et al., 2012). Treatment of plants with the hormones can mimic effects of receptor activation by pathogens(Lawton et al., 1996; Engelberth et al., 2003). The SA and JA response pathways repress each other and both repress growth (Glazebrook, 2005).

Induction of immunity of biotrophs (by SA) blocks immunity to necrotrophs, and vice versa (Thaler et al., 2012). Proteomics data could reveal hormonal pathways in algae that are activated by pathogen-produced molecules that are similar to what is seen in higher plants.

The green microalga, *Chlamydomonas reinhardtii*, contains a large group of proteins containing scavenger receptor cysteine-rich (SRCR) and C-type lectin domains which function in ligand binding and play key roles in the innate immune system of animals (Wheeler et al. 2008). Additionally, a brown macroalga, *Laminaria digitat,* and a red alga, *Gracilaria conferta,* are known to possess a mechanism of innate immunity involving pathogen attack recognition. Perception of endogenous oligosaccharides causes an oxidative burst, killing the infecting bacteria

In these alga, perception of bacterial pathogen results in the release of oligosaccharides (products from degradation of their own cell walls) causing an oxidative burst, killing the infecting bacteria (Potin et al., 2002). Algae may have developed defense mechanisms, such as a hypersensitive response, induced chemical defenses, changes in their morphology, as well as other evolutionary defense mechanisms (Kagami et al., 2007). In freshwater phytoplankton, various chemical cues have been found to be induced after mechanical damage, herbivore presence, and grazing. Other inducible defenses include formation of colonies, spines, thicker cell walls, and cysts (Van Donk et al., 2010).

Understanding on a molecular level how chytrid-like fungi interact with algae and what resistance mechanisms algae could mount to defend against infection is critical to developing a long-term biological solution to fungal infection. We performed a proteomic

interrogation of a compatible interaction (host strain is susceptible to chytrid-like fungi infection) to better understand the molecular reaction of naïve algae cells to pathogen attack. We looked at the basic molecular interactions between algae and chytrid-like fungal pathogen to identified possible proteins and/or mechanisms involved in the algal response to predation.

RESULTS

Laboratory culturing of *S. dimorphus* and chytrid-like fungi "FD61"

Chytrid-like fungi are thought to be obligate parasites (Vélez et al., 2011) and cannot be cultured on their own, therefore culturing of the parasite involves inoculation of algae and fungi in a co-culture and subsequent crash of the algal population allowing for propagation of fungal spores.

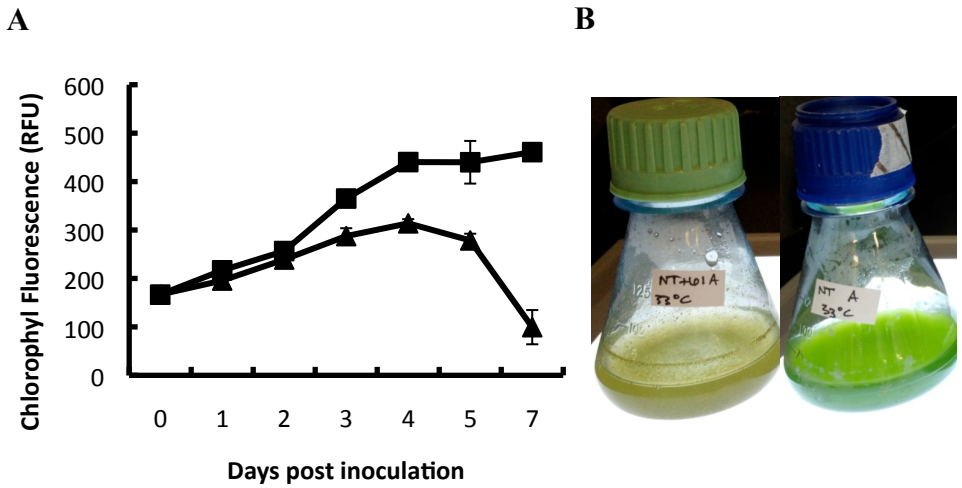

Figure 7: Algae pandemics in laboratory conditions

A) Cultures of *S. dimorphus* infected with "FD61" (▲) shows decreased chlorophyll fluorescence 3 days post infection. Non-infected controls (■) show increased chlorophyll fluorescence through the duration of the experiment. Fluorescence measured by relative fluorescence units (RFU) measured using Fluorescence micro plate reader with excitation at 450nm and emission at 680nm. Error bars are standard deviations of three biological replicates.

B) 4 days post infection with FD61 cultures (left) appear brown in color and many algal cells are agglutinated forming clumps in the culture media compared to non-infected control (right).

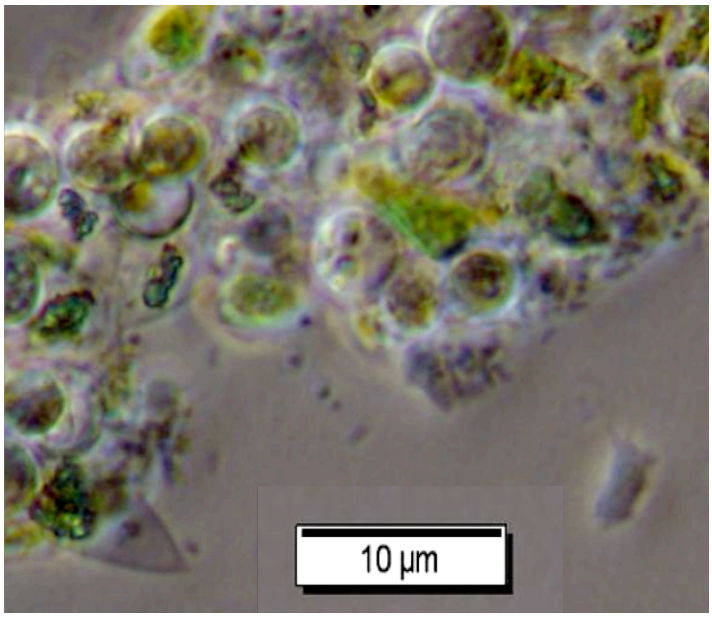

Figure 8: Chytrid spores visualized by phase contrast light microscopy

FD61 spore shown near a group of infected *S. dimorphus*. Round, transparent sporangium can be seen attached to infected *S. dimorphus* cells. Infected *S. dimorphus* cells maintain shape however green pigment is lost.

Proteomic observation of infection induced changes

In order to determine the changes occurring in the algal proteome due to infection, we set up a compatible interaction time course experiment. *S. dimorphus* cultures in triplicate were infected with FD61 and non-infected control samples in triplicate were inoculated at the same time and all flasks were incubated at 33°C. Samples were taken out for growth measurements and cultures were harvested at 1, 6, 12, 18,24, 36, and 48 hours following infection. Harvesting samples includes freezing the biomass pellet for future protein extraction for mass spectrometry. Algae growth was quantified using cell titer. FD61 growth was measured using qPCR to track target genomic DNA from the pest with primers designed from ITS1 region of FD61 as described in Letcher et al. 2013 for *Amoeboaphelidium protococcarum*.

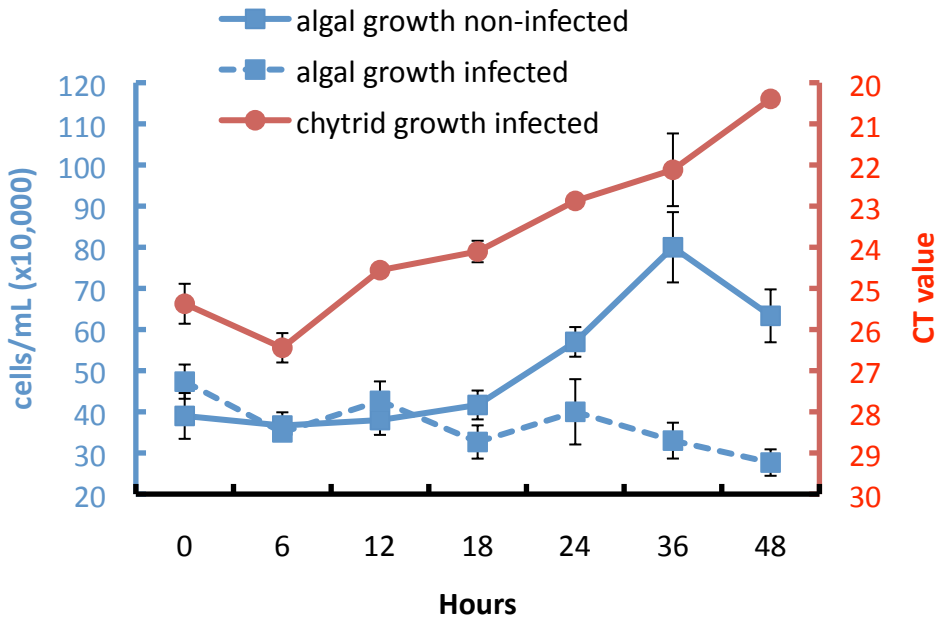

Figure 9: Culture conditions for proteomic experiment

Cultures of *S. dimorphus* infected by FD61 show gradual decrease of cell titer over time (dashed blue line, left Y axis [titer x 10, 000]) and an increase in FD61 genomic DNA (dashed red line, right Y axis [Ct (cycle threshold) value]). Non-infected controls show an increase in cell titer (solid blue line, left Y axis [titer x 10, 00]). Error bars are standard deviations of three biological replicates.

We observed cell viability decrease in infected cultures and increased in non-infected cultures over the course of the two-day experiment. Also, pest FD61 genomic DNA increased, shown by a decreasing Ct (cycle threshold) value, during the course of the experiment.

Infection induces changes in the proteome

We categorized proteins based on their expression values or abundance in the infected samples compared to non-infected controls. To determine if proteins changed in expression at a given time point between the infected (I) and non-infected (NI) sample we

calculated an average of the expression values from the biological replicates for each condition (I, NI) and time point. (N.B. Each biological replicate is the average of two technical replicates). From the average expression value we calculate an ratio of infected: non-infected (I:NI). Based on this ratio, proteins were categorized as increased, ratio > 1.5, or decreased, ratio <0.6, in abundance. We observed 1213 proteins increased abundance and 834 proteins decreased abundance due to infection.

Table 1: Proteins change in abundance after infection

The number of proteins changed (during at least one time point) after FD61 infection of *S. dimorphus*. Comparing infected to non-infected samples 1213 proteins showed increased abundance (ratio >1.5) and 834 proteins showed decreased abundance (ratio <0.6).

Proteins measured	2,546
Changes after infection	1213 Increased 834 Decreased
Selected for further research	11

Heat map showing protein expression pattern over time

In this study we used weighted correlation network analysis (WGCNA) to find clusters of highly correlated proteins. This type of analysis can be useful in filtering large data sets for groups of proteins behaving similarly throughout the course of the experiment (Langfelder and Horvath, 2008). Data generated from iTRAQ labeled mass spectrometry is reported as "reporter ion intensities" values, representing the 4-iTRAQ reagents (114, 115, 116, and 117) used to label peptides in various sample types and a threshold of 500 was set for individual intensity values. Coefficient of variance (CV) was computed for technical replicates and only those with CV below 0.5 were included. All individual reporter ion (114, 115, 116, 117) intensities were averaged with the same

intensities from the other biological replicates. From this a ratio of intensities of infected to non-infected was calculated in order to compare protein abundance in different sample types. These ratios were used to generate a matrix showing the correlation between different proteins at different time points. This matrix was used to create a gene dendrogram, which shows modules of proteins that are being expressed similarly and a heat map as a graphical representation where individual values in a matrix are represented as colors (red and blue).

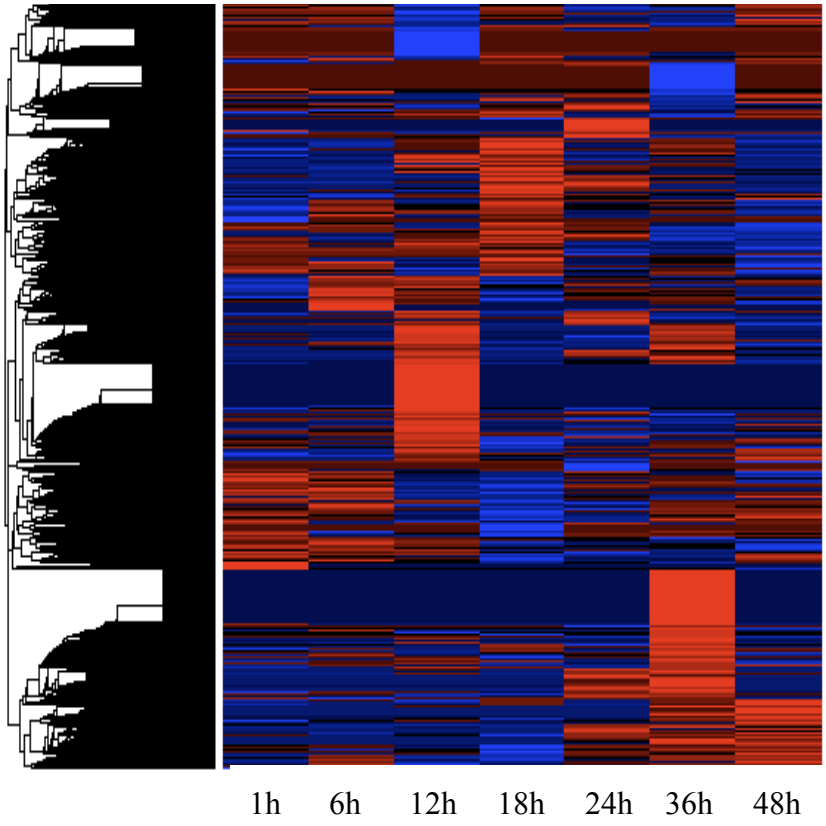

Figure 10: Heat map showing protein expression pattern over time

Hierarchical clustering analysis of expression patterns of all proteins perceived by mass spectrometry experiments involving exposure of *S. dimorphus* to FD61 chytrid-like fungi. Red represents proteins increased in abundance (ratio >1.5) and blue represents proteins decreased in abundance (ratio <0.6) in infected samples compared to non-infected.

Plant defense homologs induced after infection

We utilized MapMan (Thimm et al., 2004) to perform functional annotation of the proteins quantified in mass spectrometry analysis. We focus on proteins that are known to play a role in plant defense to see if they are detected in infected samples and we hypothesize they change in abundance in infected samples compared to non-infected samples.

Based on MapMan functional annotation, we identified 11 proteins showing homology to proteins known to be involved in plant defense. These particular 11 proteins show significant change in expression due to infection. As previously mentioned, the data was calculated as a ratio of infected: non-infected expression values. These ratios were log2 transformed i.e. if protein expression doubles (ratio = 2.0) the log 2 expression ratio is equal to 1.0 while if protein expression is halved (ratio=0.5) the log2 expression ratio is equal to -1.0.

Infection induces receptor like kinase leucine rich repeat

Mass spectrometry analysis reveals a protein homologous to a leucine rich repeat receptor like kinase (LRR-RLK) in *A. thaliana.* Figure 11 shows LRR-RLK homolog increases abundance by 1.4-fold ($p<0.05$) 12 hours after infection and by 1.3-fold ($p<0.1$) 36 hours after infection.

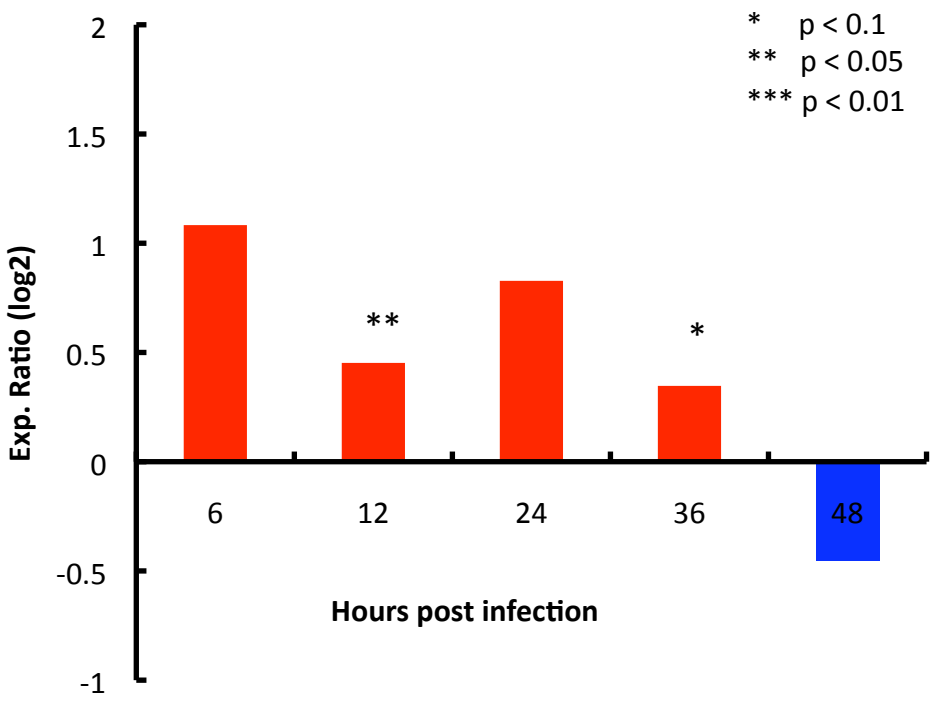

Figure 11: Infection induces a leucine-rich repeat receptor like kinase

Expression of a protein homologous to receptor-like kinase leucine rich repeat (RLK-LRR) is observed. Expression ratios calculated for the protein at each time point after infection (x-axis) is calculated to compare the protein abundance in infected samples versus to non-infected samples and this ratio is reported (log2 transformed) on the y-axis. This RLK-LRR like protein is significantly increases abundance 12 hours ($p<0.05$) and 36 hours ($p<0.1$) post infection.

Infection induces algal cell agglutination

One of the phenotypes *S. dimorphus* displays following chytrid infection is cell agglutination, which forms clumps in the media. In this experiment we show cell agglutination 12 hours after infection with chytrids.

Figure 12: Infection induces algal cell agglutination 12 hours after infection

Non-infected cultures (left flask) do not contain agglutinated algal cells. Infected cultures (right flask) show agglutinated cells, forming clumps in the media. Picture was taken 12 hours after infection.

Mass spectrometry analysis reveals three proteins homologous to *A. thaliana* Fasciclin-like arabinogalactin (FLA) proteins. Figure 13 (A) shows FLA11 homolog increases abundance by 1.6-fold ($p<0.05$) 6 hours after infection. Figure 13 (B) shows FLA12 homolog increases abundance by 2.0-fold ($p<0.01$) 6 hours after infection. Figure 13 (C) shows FLA17 homolog decreases abundance by 0.5-fold ($p<0.05$) 48 hours after infection.

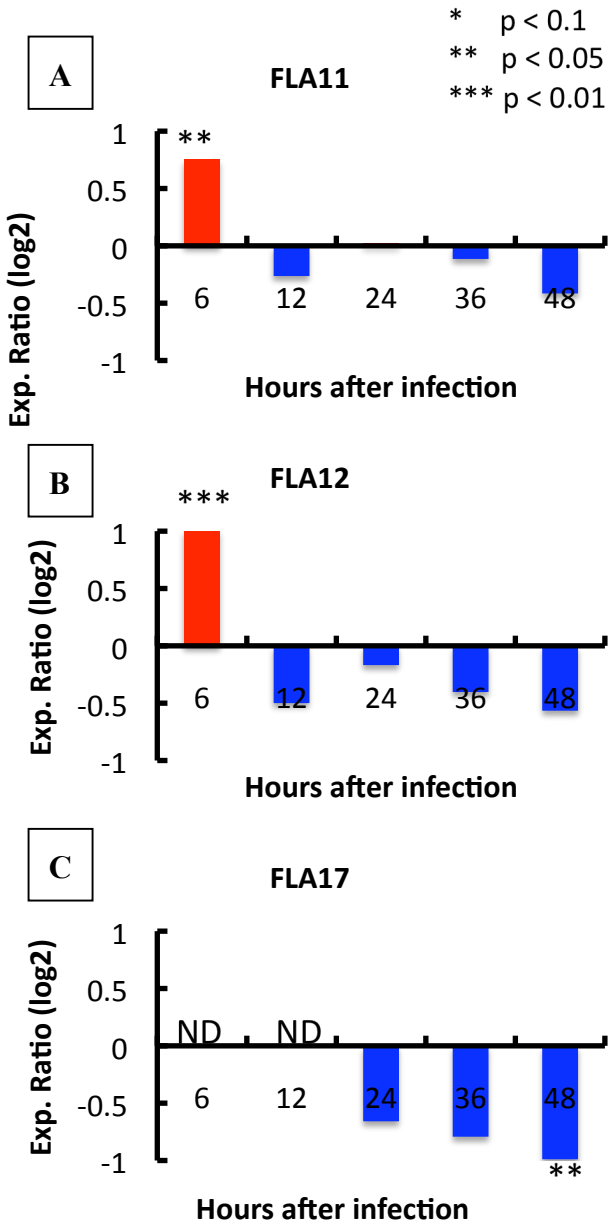

Figure 13: Infection transiently expresses three fasciclin-like proteins

Expression of a protein homologous to fasciclin like proteins FLA11, 12, and 17 are observed. Expression ratios calculated for the protein at each time point after infection (x-axis) is calculated to compare the protein abundance in infected samples versus to non-infected samples and this ratio is reported (as log2) on the y-axis. A) FLA11 significantly increases abundance 6 hours ($p<0.05$) after infection. B) FLA12 also significantly increases in abundance 6 hours ($p<0.01$) after infection. C) FLA17 significantly decreases abundance 48 hours ($p<0.05$) after infection.

Infection induces a cinnamyl alcohol dehydrogenase

Mass spectrometry reveals a protein homologous to a cinnamyl alcohol dehydrogenase (CAD) in *A. thaliana*. Figure 14 shows CAD homolog increases abundance by 2.2-fold ($p<0.1$) 12 hours after infection and increases abundance by 1.7 fold ($p<0.1$) 36 hours after infection.

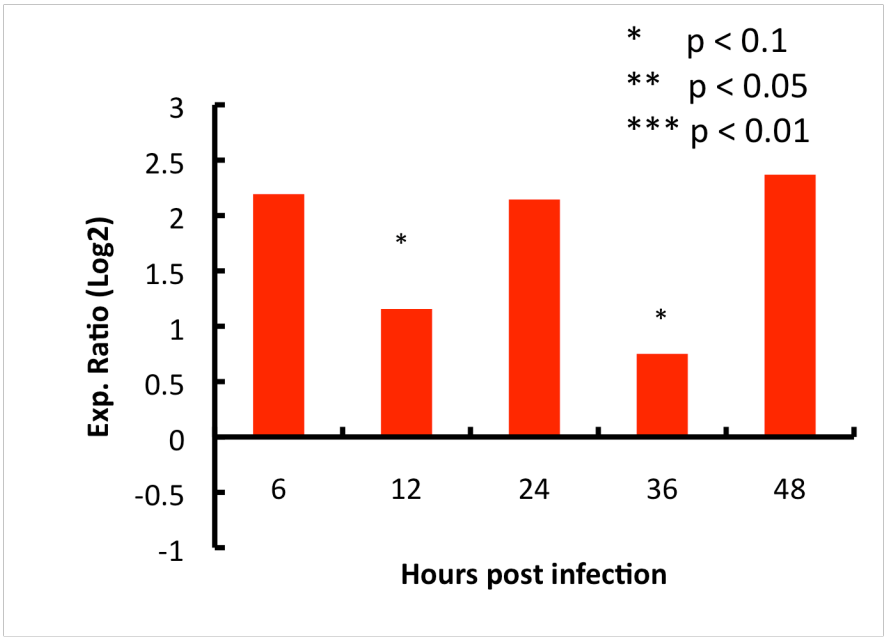

Figure 14: Infection induces cinnamyl alcohol dehydrogenase

Expression of a protein homologous to cinnamyl alcohol dehydrogenase (CAD) is observed. Expression ratios calculated for the protein at each time point after infection (x-axis) is calculated to compare the protein abundance in infected samples versus to non-infected samples and this ratio is reported (as log2) on the y-axis. CAD significantly increases abundance 12 hours ($p < 0.1$) and 36 hours ($p<0.1$) after infection.

Infection induces shikimate pathway enzymes

Four of six enzymes in the shikimate pathway were revealed through mass spectrometry analysis. Figure 15 (A) shows 3-deoxy-7phosphoheptulonate synthase (DHAP) homolog increases in abundance by 1.4-fold ($p<0.05$) 36 hours after infection. Figure 15(B) shows shikimate kinase homolog increases abundance by 2.5 fold ($p<0.1$) 6 hours after infection. Figure 15 (C) shows 5-enolpyruvylshikimate-3-phosphate synthase

(EPSP) homolog increases abundance by 2.0-fold ($p<0.1$) 6 hours after infection. Figure 15 (D) shows chorismate synthase homolog increases abundance by 1.2-fold ($p<0.1$) at both 12 and 36 hours after infection.

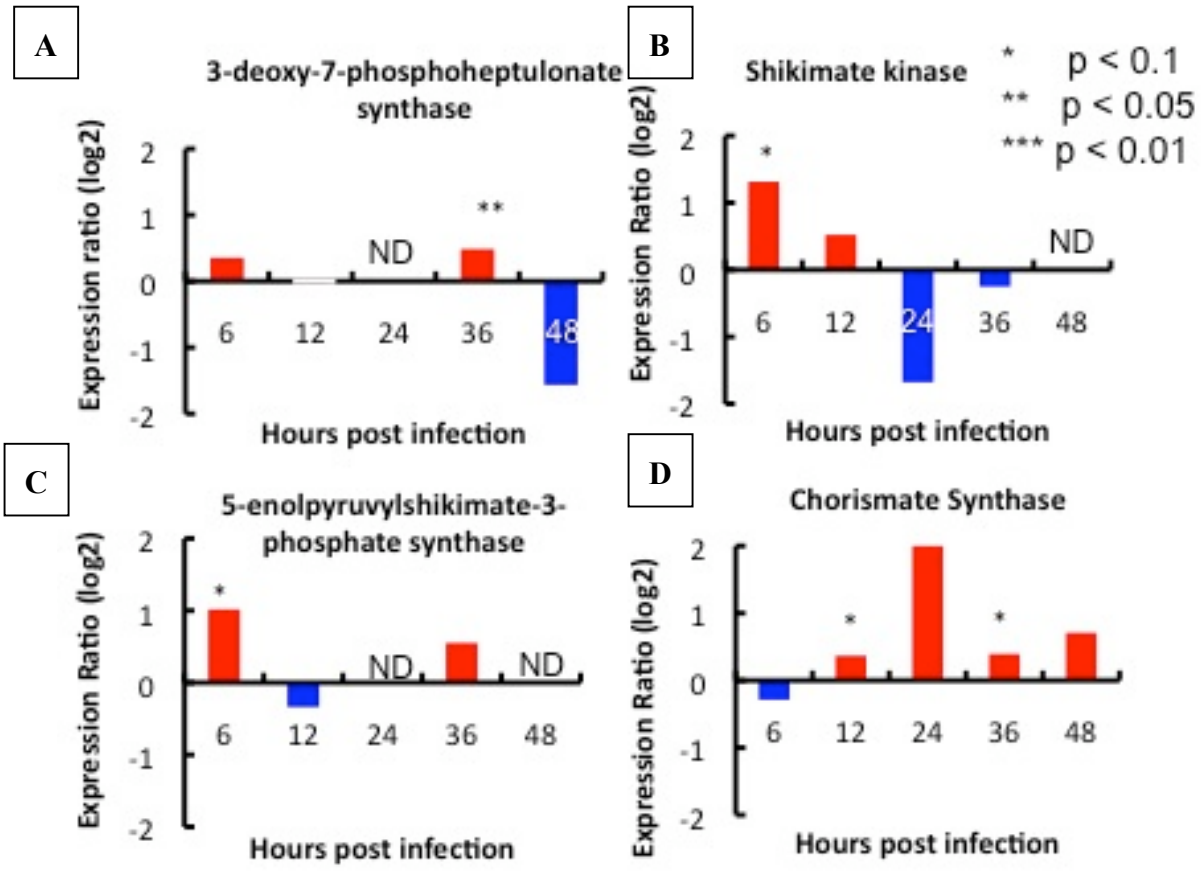

Figure 15: Infection induces four enzymes in shikimate pathway

Expression of proteins homologous to four enzymes involved in shikimate pathway is observed. Expression ratios calculated for the protein at each time point after infection (x-axis) is calculated to compare the protein abundance in infected samples versus to non-infected samples and this ratio is reported (as log2) on the y-axis. A) 3-deoxy-7-phosphoheptulonate synthase significantly increases abundance ($p<0.05$) 36 hours after infection. B) Shikimate kinase significantly increases abundance ($p<0.1$) 6 hours after infection. C) 5-enolpyruvylshikimate-3-phosphate synthase significantly increases abundance ($p<0.1$) 6 hours after infection. D) Chorismate synthase significantly increases abundance ($p<0.1$) 12 and 36 hours after infection.

Infection induces a tryptophan synthase

Mass spectrometry analysis reveals a protein homologous to tryptophan synthase, an enzyme involved in synthesis of tryptophan. Figure 16 shows a tryptophan synthase homolog increases in abundance by 2.4-fold ($p<0.1$) 36 hours after infection.

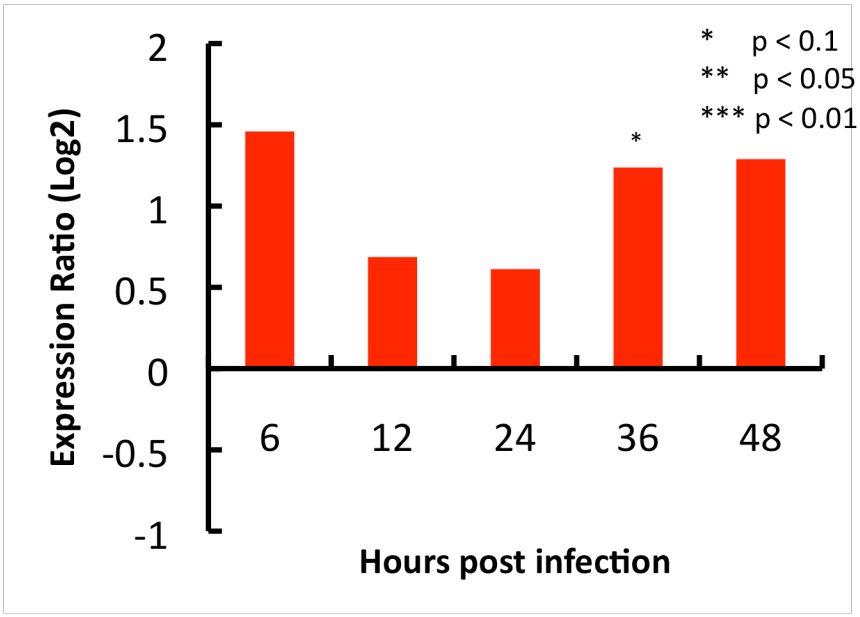

Figure 16: Infection induces a tryptophan synthase

Expression of proteins homologous to a tryptophan synthase is observed. Expression ratios calculated for the protein at each time point after infection (x-axis) is calculated to compare the protein abundance in infected samples versus to non-infected samples and this ratio is reported (as log2) on the y-axis. Tryptophan synthase significantly increases abundance ($p<0.1$) 36 hours after infection.

Infection induces a jasmonic acid biosynthetic enzyme

Mass spectrometry data reveals a protein homologous to lipoxygenase (LOX3) in *A. thaliana*. LOX3 is necessary for synthesis of plant hormone Jasmonic Acid. Figure 17 shows LOX3 homolog increases abundance by 1.3-fold ($p<0.01$) 36 hours after infection.

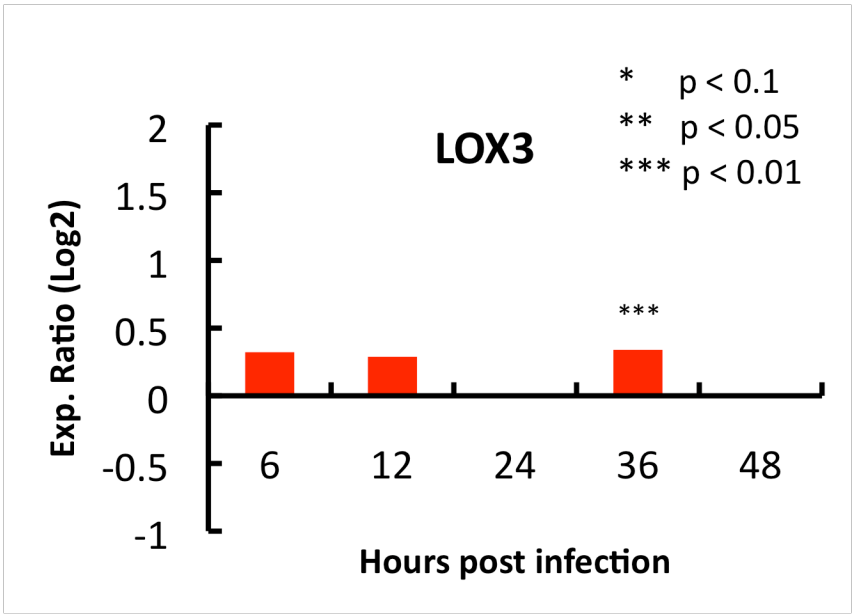

Figure 17: Infection induces a jasmonic acid biosynthetic enzyme

Expression of proteins homologous to lipoxygenase (LOX3), a jasmonic acid biosynthetic enzyme is observed. Expression ratios calculated for the protein at each time point after infection (x-axis) is calculated to compare the protein abundance in infected samples versus to non-infected samples and this ratio is reported (as log2) on the y-axis. LOX3 significantly increases abundance ($p<0.01$) 36 hours after infection.

BTH, meJA treatment alters FD61 infection phenotype

Figure 18 shows the chlorophyll flurosence for non-infected *S. dimorphus* samples treated with BTH, meJA, or DMSO (control). Fluorsence for all samples increases at the same rate over the course of the experiment. Thus BTH and meJA treatment does not affect non-infected growth of *S. dimorphus*.

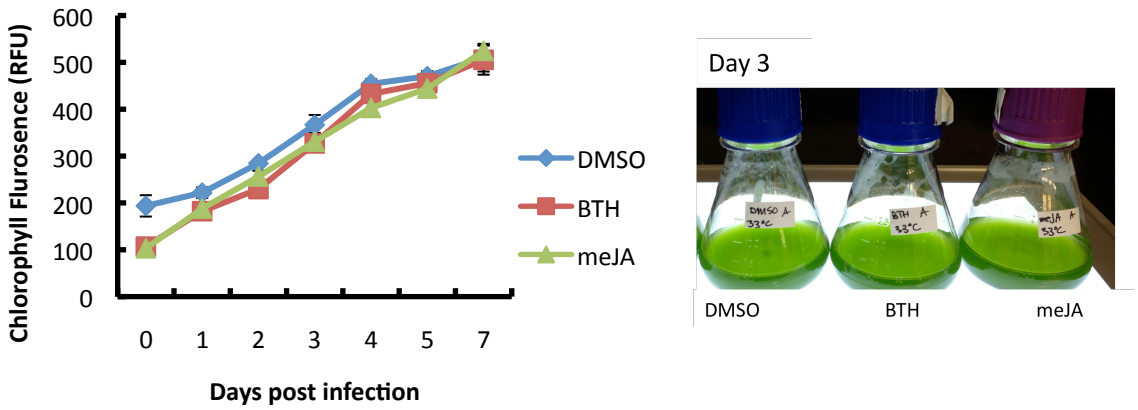

Figure 18: BTH, meJA does not affect non-infected culture growth

Cultures of *S. dimorphus* treated with 100uM BTH (red line), 100uM meJA (green line) and control DMSO (blue line)). Cultures treated with BTH, meJA, and control DMSO all increase fluorescence over the period of the experiment. Picture taken of culture flasks on day 3: DMSO control (left) and BTH treated (middle) and meJA (right).

Figure 19 shows the chlorophyll flurosence for infected samples pretreated with BTH, meJA, or DMSO (control). Flurosence decreases in meJA treated samples 1 day post infction, fluoresence decreases in BTH treated samples 2 days post FD61 infection. While fluorsence decreases in control samples 3 days post FD61 infection. Thus treatment with meJA and BTH accelerates FD61 infection phenotypes.

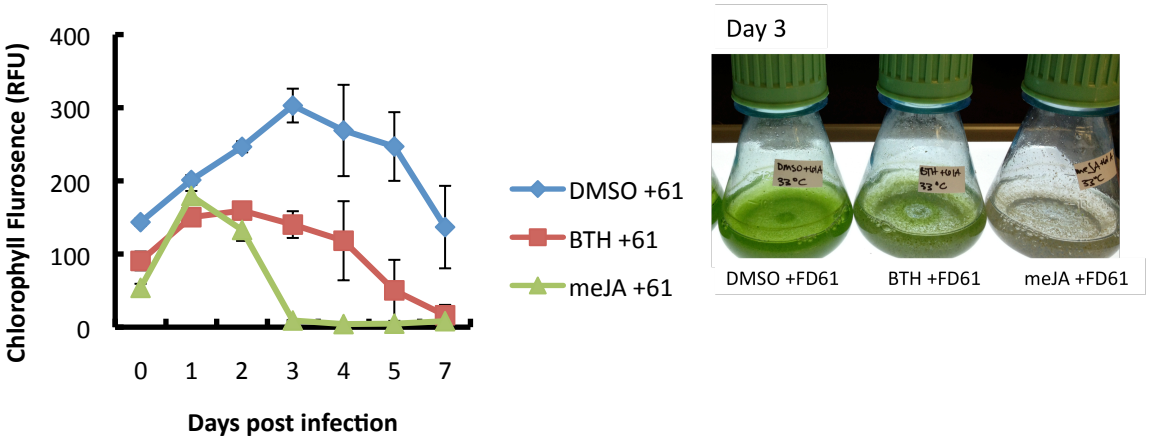

Figure 19*:* BTH, meJA accelerate FD61 infection

Cultures of *S. dimorphus* treated with 100uM BTH (red line), 100uM meJA (green line) and control DMSO (blue line)) and infected with FD61. Cultures treated with meJA decrease in chlorophyll fluorescence 1-day post infection. Cultures treated with BTH decrease in chlorophyll fluorescence 2 days post infection. DMSO control cultures decrease in chlorophyll fluorescence 3 days post infection. Thus meJA and BTH accelerate FD61 infection of *S. dimorphus*. Picture taken of culture flasks on day 3: DMSO control (left) and BTH treated (middle) and meJA (right).

BTH, treatment alters FD01 infection phenotype

Figure 20 shows the chlorophyll flurosence for infected samples pretreated with BTH, meJA, or DMSO (control). Fluorsence decreases in meJA treated samples 3 day post infction, fluorsence decreases in BTH treated samples 4 days post FD01 infection. While fluoresence decreases in control samples 3 days post FD01 infection. Thus BTH treatment of *S. dimorphus* delays FD01 infection and meJA accelerates FD01 infection phenotype.

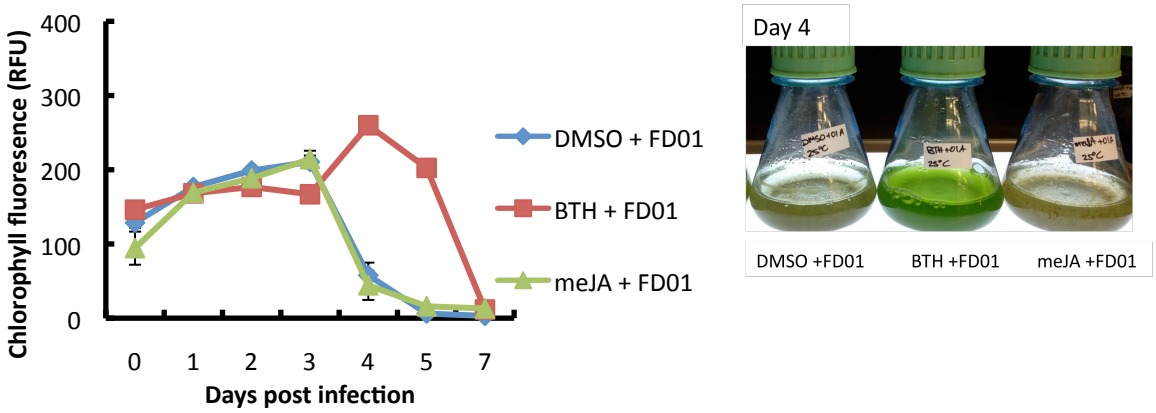

Figure 20: BTH delays FD01 infection

Cultures of *S. dimorphus* treated with 100uM BTH (red line), 100uM meJA (green line) and control DMSO (blue line)) and infected with *A. protococcarum*. Cultures treated with BTH show decreased chlorophyll fluorescence 4 days post infection. meJA and control cultures show decreased chlorophyll fluorescence 3 days post infection. Thus BTH delays A. protococcarum infection of *S. dimorphus* by 1 day. Picture taken of culture flasks on day 4: DMSO control (left) and BTH treated (middle) and meJA (right).

Genetic screen for mutants

A mutant library containing ~400,000 mutants was created using nuclear transformation of linearized plasmid DNA. Pale color mutants were isolated from the library. The pale mutants provide further verification that our transformations were successful in producing mutations that cause a change in phenotype.

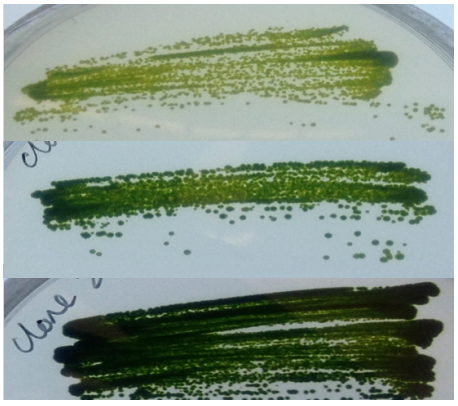

Figure 21: Pale mutants isolated from gene-disruption library

Mutants isolated from library showed different color phenotypes. Light green (first streak), green (second streak), and dark green (third streak) color phenotypes were observed.

DISCUSSION

Algae as biomass producers

The goal of this research project is to understand how microalgae respond to infection. Algae have shown serious potential as a biofuel crop as they can produce lipids which can be converted into fuel (Jones and Mayfield, 2012). In order to become realistic alternative to fossil fuels, it must become economically viable to cultivate the algae, which currently is most feasible in large, outdoor raceway ponds. Like many agriculture crops grown on a large scale, these organisms are susceptible to many different factors in the environment, both abiotic and biotic. *Scenedesmus* is a potential biomass crop with relatively high lipid accumulation of ~26% (Mandal and Mallick, 2009; Prabakaran and Ravindran, 2012) and can tolerate high temperatures up to 30C (Li et al., 2011). However it is susceptible to infection by parasitic chytrid-like fungi. These parasitic fungi have been isolated from *Scenedesmus* ponds and methods have been developed for culturing in lab conditions (Letcher et al., 2013). There is very little known about how the algae respond on a molecular level to this infection. Our focus was to investigate the changes in the algal proteome in response to infection by a pathogenic chytrid-like fungus.

Large-scale agriculture is heavily dependent on phenotype of a particular crop. Desirable phenotypes can include tolerance to environmental stress such drought, high salinity, high temperatures, and pathogen attack (e.g. bacteria, viruses, and fungi). Contrary to the genotype, proteotype is also influenced by the developmental stage of the organism and the environment and proteotype directly influences the phenotype. Therefore proteomics is the best method to study changes in *S. dimorphus* after chytrid-like fungi infection.

Use of mass spectrometry to identify and quantify changes due to infection

iTRAQ reagents were used to label samples to enable analysis of infected and non-infected samples in one mass spectrometry run. In each biological replicate contained two technical replicates that were each labeled with a separate iTRAQ reagent. Two non-infected samples (labeled with iTRAQ reagents 114, 115) and two infected samples (iTRAQ reagents 116, 117) were combined into one mass spectrometry run (therefore there are two technical replicates per biological replicate sample). This was repeated for each biological replicate and at each time point analyzed. Identical peptides derived from different samples have the same mass. However, with iTRAQ labeling, the signal intensity ratios of the reporter groups of the isobaric tag indicate the ratios of the peptide quantities and can be used to determine the relative quantities of the peptides. Therefore iTRAQ is ideal to compare samples coming from different treatments (e.g. infected and non-infected)

Proteins differentially expressed following infection

In this study we found over 2,500 proteins with differential expression after infection. There were 1213 proteins over expressed and 834 proteins under expressed in at least one time point. 263 proteins were both over and under expressed and 756 proteins were unchanged throughout the course of the experiment (**Table *1***).

Plants can recognize pathogens through extracellular and intracellular receptors which both signal to modulate immune responses reviewed in Bonardi and Dangl, 2012. Leucine rich repeat receptor like kinases (LRR-RLK) are proteins located at the cell surface with extracellular, transmembrane, and serine/threonine kinase domains. LRR-

RLKs are involved in plant defense and development. LRR-RLKs perceive pathogen presence and relay downstream signals that mediate a defense response. Intracellular receptors include the nucleotide binding (NB) domain leucine-rich repeat (LRR) protein family which play an important role in defense response in plants. NB-LRRs have been shown to exist across kingdoms and seem to act in similar ways as mediators of immune response reviewed in (Bonardi and Dangl, 2012). It has been shown in plants that many of the innate immune receptors and disease resistance (R) proteins contain NB-LRR domains and the largest class of R proteins contains NB-LRR domains. NB-LRR type proteins have also shown homology to intracellular signaling domains of Drosophila (Toll) and mammalian (interleukin-1) receptor proteins (Dangl and Jones, 2001). Plants are known to recognize plant effector molecules through these R proteins and target other components of effector-triggered immunity (ETI), which includes R protein signaling downstream to induce a hypersensitive response (HR) or programmed cell death (PCD). We observed increased expression of a protein homologous to A. thaliana LRR-RLK at two different time points after infection (**Figure *11***). This receptor protein could be involved in *S. dimorphus* recognition of the chytrid pathogen.

Agglutination a possible defense mechanism

Algae have shown inducible defenses including colony forming to avoid grazing by small zooplankton. It is suggested that this is an adaptive response to reduce predation (Van Donk et al., 2010). Additionally, *Scenedesmus* has been shown to display another type of adaptive response; algal exposure of toxic compound microcystin is followed by the release extra-cellular and intra cellular polysaccharides (El-Sheekh et al., 2012).Fasciclins are putative cell adhesion domains. Fasciclin domains have been shown

to be involved in cell adhesion during development of multicellular green alga *Volvox cateri* (Huber and Sumper, 1994). Fascicilin-1 domains belong to the group of arabinogalactin proteins found throughout eukaryotic organisms (Harwood and Coates, 2004). Genome analysis of *Chlamydomonas reinhardtii* revealed cell-cell adhesion domains hypothesized to have played a role in the transition to multicellular existence. (Wheeler et al., 2008). In wheat, a proteomic study revealed a FLA protein was induced after H_2O_2 stress (Ge et al., 2013). Shortly after infection in laboratory conditions, algae cells agglutinate forming clumps in the culture (**Figure *12***). We observed infected samples showed over expression of a protein with homology to fasciclin-like domains (**Figure *13***). It is possible that *S. dimorphus* flocculates in order to protect themselves from pathogens as this could be a way to elude predators in nature. We hypothesize that these FLA proteins could be involved in a *S. dimorphus* defense response.

Plant defense homologs induced after infection

In plants, phenylpropanoids have been shown to have anti-microbial properties that are constitutive and induced (La Camera et al., 2004). Additionally, genome-wide analysis of the phenylpropanoid pathway showed these predicted phenylpropanoid pathway genes are present in 11 plant species (Naoumkina et al., 2010). We also observed a protein homologous to phenylpropanoid, cinnamyl alcohol dehydrogenase (CAD) is over expressed in infected samples compared to non-infected samples (**Figure *14***).

Of these differentially expressed proteins, we found a group of proteins homologous to *A. thaliana* proteins in the shikimate pathway, which synthesizes chorismate. Chorismate is an important biochemical intermediate in plants and precursor

to many important molecules in plants including Aromatic Amino Acids (AAAs). AAAs are involved in the synthesis of many different natural products including hormones, pigments, alkaloids, and cell wall components in plants (Maeda and Dudareva, 2012). One important product of chorismate is the plant hormone salicylic acid (SA). Upon recognition of biotrophic pathogens, SA is induced and activates expression of pathogenesis-related (PR) genes inducing disease resistance.

We observed a group of proteins homologous to enzymes in the *A. thaliana* shikimate pathway. We found four of the six enzymes in the shikimate pathway and all four of these enzymes were significantly over expressed following infection (**Figure *15***). These enzymes could be induced in *S. dimorphus* after infection by chytrids as a defense response. Since chytrids are obligatory parasites of algae, they could be biotrophic pathogens of the algae. In plants, SA mediated defense response is triggered after perception of a biotrophic pathogen.

Chorismate is also a precursor to the amino acid tryptophan. *A. thaliana* mildew resistance locus 2 (mlo2) mutants accumulated tryptophan metabolites that were required for antifungal defense (Consonni et al., 2010). We found that a protein homologous to tryptophan synthase was over expressed after infection (**Figure *16***). Tryptophan synthase may be involved in mediating a defense response in *S. dimorphus* after chytrid infection.

Although we detected multiple enzymes in the shikimate pathway, including Chorismate synthase, we did not detect any proteins homologous to the enzymes that catalyze synthesis of salicylic acid from chorismate. As mentioned previously, in plants SA mediated defense is antagonized by JA. Interestingly, we observed an increase in abundance by 1.2 fold ($p=0.002$) of a homolog to lipoxygenase (LOX), which catalyzes

the synthesis of Jasmonic acid (**Figure *17*)** One possible explanation for this increased in abundance of a JA-related protein is that JA is suppressing SA production, and thus without SA, the fungal infection persists.

Plant biotic stress hormones

In *A. thaliana* the SA mediated defense pathways can be induced by treatment with BTH (benzo(1,2,3) thiadiazole-7-carbothioc acid S-methyl ester), a SA synthetic analog. Plants pre-treated with BTH show less susceptibility to biotrophic pathogen compared to the non-treated ((Lawton et al., 1996).

We are interested in finding if plant defense hormones, particularly SA and JA, play a role in algae response to infection. To this end we treated *S. dimorphus* with BTH (100uM) and methyl jasmonate (100uM) for 36 hours and then inoculated the cultures with chytrid infection sources FD61 and *A. protococcarum*. BTH and meJA treatment both accelerated infection phenotypes by FD61. BTH treatment delayed infection by FD01 while meJA treatment accelerated infection by FD01. We see that the affects of hormone treatments are variable depends on the infection source. It is possible that the affects we've seen from the hormones on infection could be dependent on the concentration of hormone treatment as well as time of treatment. In another experiment (results not shown) hormone treatment impaired non-infected culture *S. dimorphus* growth. The results showing BTH and meJA treatment altering *S. dimorphus* response to chytrid infection suggests plant hormone SA and JA pathways, known to be involved in plant defense response to infection, may be conserved in the green alga.

To further test the hypothesis that plant defense hormone pathways are conserved in *S. dimorphus* we created a gene disruption mutant library. The mutant library was

created by performing nuclear transformation and generating ~400,000 mutants which should be sufficient to cover the genome of *S. dimorphus*. With this library we plan to perform a screen to find mutants less susceptible to SA and JA hormones. These mutants would then be tested for susceptibility to chytrid infection. We hypothesize that mutants who are more resistant to JA will be less susceptible to *A. protococcarum* infection and mutants more resistant to SA will be more susceptible to *A. protococcarum* infection.

MATERIALS AND METHODS

Algae and parasite culture conditions

Axenic cultures of *S. dimorphus* (UTEX 1237, University of Texas Culture Collection of Algae, http://web.biosci.utexas.edu/utex/) were grown at 25˚C on a shaker (150 rpm) in an acrylic box with continuous light (Utilitech Lighting 4100 K T8 light bulbs, ~200 microEinsteins) and were provided 100% CO_2 at a flow rate of 0.2 L/min. *S. dimorphus* was grown in modified artificial seawater media [MASM(D)]. MASM(D) was prepared by dissolving 1.0 g tris, 2.49 g magnesium sulfate heptahydrate, 1 g sodium bicarbonate, 0.6 g potassium chloride, 1.0 g sodium nitrate, 0.3 g calcium chloride dihydrate, 0.05 g potassium phosphate monobasic, and 6 mL *Closterium* Medium trace elements (1 g sodium EDTA, 0.194 g ferric chloride, 0.072 g manganese chloride, 0.021 g zinc chloride, 0.013 g sodium molybdate, and 0.004 g cobalt (II) chloride into 1 L DI H_2O, sterilized using a Corning 0.22 μM filter system).

Algal parasite, FD61, was present in samples of *S. dimorphus* grown in outdoor cultivation ponds, isolated using plaquing techniques, and identified using qPCR as described in Letcher et al (2013). FD61 pure cultures were harvested from frozen DMSO stock, inoculated into cultures of *S. dimorphus* in 125mL disposable flasks, starting Optical Density (OD) 0.1, 750nm, 200uL sample measured using micro plate reader. Infected culture flasks were placed in acrylic box maintained at 33-34°C, 2% CO_2, ambient light, and shaking at 100 rpm.

Pest FD61 was isolated from outside ponds in Sapphire outdoor ponds in Las Cruces, NM. For the purpose of propagating cultures of FD61, cultures of *S. dimorphus*, monitored for optical density (OD) at 750nm using 200uL volume in a micro plate

reader, were diluted to final OD 0.1 and then infected with the pest and maintained at 33-34˚C with continuous light.

Algae growth assays

Cell viability and chlorophyll fluorescence measurements were used as proxies for algal growth. Titer assay was performed by plating 10 µL aliquots from a ten-fold serial dilution on G0 agar plates. GO media was prepared by dissolving in 1L of water $MgSO_4$ 406mM, $CaCl_2$ 47 mM, H_3BO_3 162 mM, $NaVO_3$ 2.1 mM,0.5 g of bicarbonate $HC0_3$, 1.29 ml of F/2A trace elements and of F/2B Vitamin Mix. Media was then sterilized by using a Corning 0.22 µM filter system. F/2A trace element is prepared by dissolving 4.36 g of Na2EDTA, 3.15g of FeCl2-6H20, 0.01g CuSO4-5H20, 0.022g of ZnSO4-7H20, 0.18g of MnCl2 in 1 L DI H_2O, by adjusting to pH8 and by autoclaving the solution for 15 minutes. F/2B vitamin Mix is prepared by dissolving 0.0005g of Cyanocobalamin, 0.1g of Thiamine HCl, 0.0005g of Biotin into 1 L DI H_2O, by adjusting to pH8 and by autoclaving the solution for 15 minutes. Plates were placed on a shelf in ambient light maintained at 25°C. Colonies were generated usually in 4-6 days.

Fluorescence plate reader was used to monitor growth by measuring increases or decreases in chlorophyll fluorescence. Chlorophyll fluorescence were measured on samples from a ten-fold dilution and read in 96-well transparent plates using a Bio-Mek Beckman counter (city, country) fluorescence plate reader. Chlorophyll fluorescence readings with the indicated excitation/emission filters (excitation 450nm, emission 680nm) were acquired using the calculated optimal gain setting. MASM(D) medium was used as a blank.

Parasite growth tracked by qPCR

DNA from pest FD061 was extracted and amplified to track level of the gDNA of the pest among the infection time, similarly as described in Letcher et al. (2013). The primers (5' to 3') used were: ITS1+2 forward GATCAAAACCGCTCACCAAT, ITS1+2 reverse TGAATTGCAGAACTCCGTGA. 50uL of sample culture was added to 50uL DNA lysis buffer (0.25X) in 96-well PCR plates. DNA lysis buffer (1X) contained 50mM Tris-HCl (pH 8.0), 200mM NaCl, 20mM EDTA(pH 8.0), 1.0% (v/v) SDS, which was diluted 1:4 with sterile water. Sample culture and lysis buffer were boiled with the following conditions: Step 1: 95°C 10:00, Step 2: 25°C 5:00, Step 3: 95°C 10:00, Step 4: 25°C 5:00, Step 5: 4°C infinite hold. Boiled samples were diluted 1:20 with sterile water. qPCR reactions were set up in 96-well plates with the following reaction mixture: 5uL SsoFast Eva Green SuperMix (Bio-Rad, #172-5201), 2.4uL 1uM primer mix (0.5uM each), 2.6uL DNA template (1:20 diluted). Reaction mixture (10uL each) were mixed and the 96-well plate was spun 2,5000 rpm, 2:00. Cycle conditions were the following: 98°C 2:00, 40X (98°C 0:01, 57°C 0:04).

Samples preparation for Mass Spectrometry

SE0004 cultures destined to protein extraction was inoculated at OD~0.2 into 500mL flasks in triplicates for both the control and 20% infection and for each time point. An FD61 fungus infection source of 20 %v/v was generated by spinning down 100 mL of infected sources and re-suspending it in 5 mL of fresh MASM(D) media. Infected and non-infected samples were then incubated at ~33°C and collected by centrifugation at the following time point: 1,6, 12, 18, 24 and 48 hours post infection.

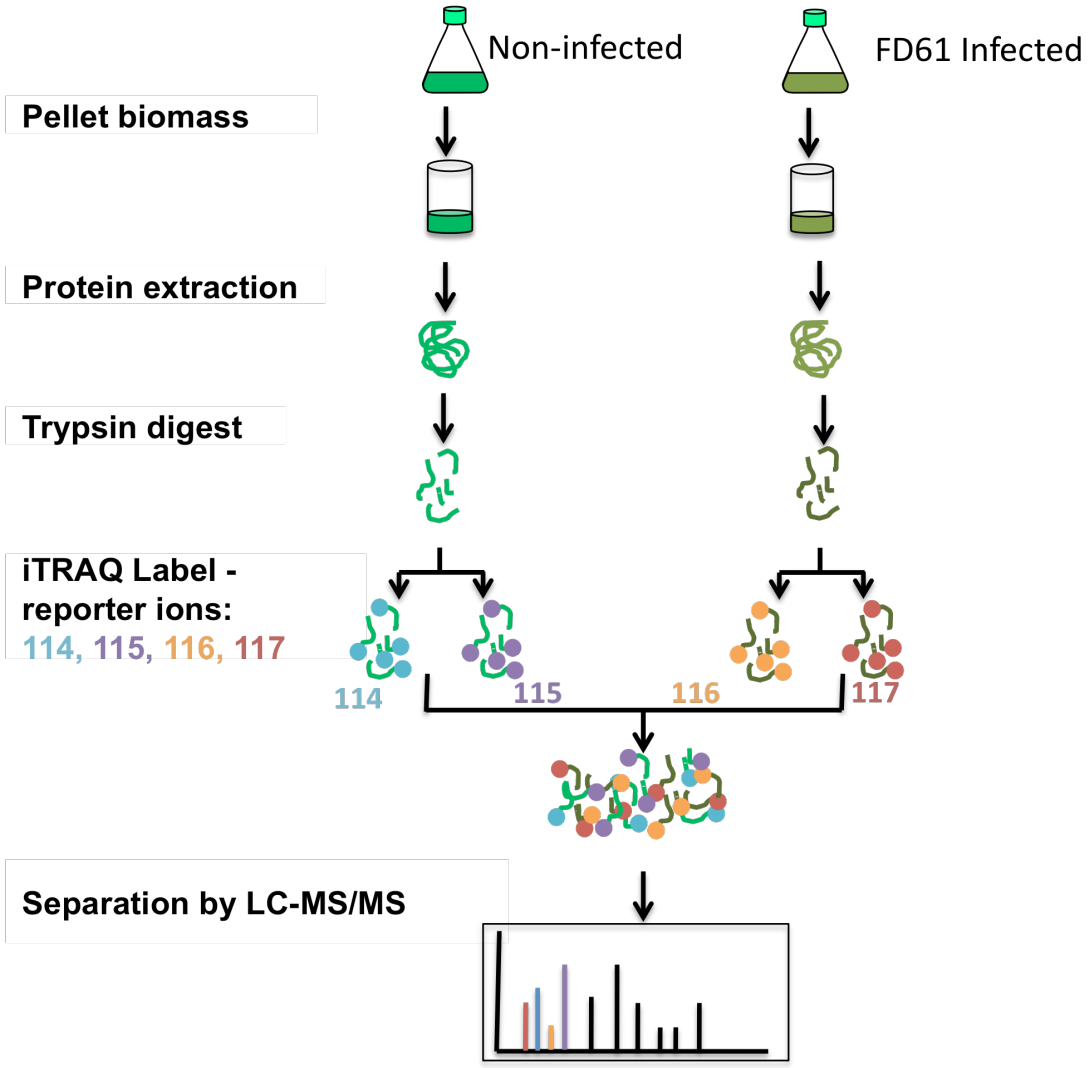

Figure 22: Experimental work flow for mass spectrometry sample preparation

Cultures were inoculated in triplicate (represented by flask on right) with *S. dimorphus* and FD61 infection source. Non-infected cultures were also inoculated in triplicate (represented by left flask). At each time point, both infected and control cultures were spun down and the biomass pellet was flash frozen using liquid nitrogen. Proteins were extracted from biomass pellet and digested into peptides using trypsin. Peptides were labeled with iTRAQ reagents. Samples were run on LC/MS/MS and resulting spectra were analyzed for identification and quantification.

Protein extraction for Mass Spectrometry

Cell pellet was resuspended in a Lysis Buffer constituted of 2% SDS in 50 mM HEPES (1:1 (v:v)), and boiled for 15 min. Cells were then lysed by 5 cycles of snap freezing, thawing and sonication Branson Sonifier for 1 minute at 30Hz. Several washes of the pellet with methanol (50 mL of MeOH with 0.2mM $Na3VO_4$ for - 30 min at -20°C) followed by washes in 100% Acetone (50mL of Acetone for 30 min at -20C) were performed until photosynthetic pigments were removed from the pellet/supernatant.

Pellet was resuspended in two times volume of a 1% SDS in 50mM Hepes/1mM EDTA/ solution/1mM TCEP (pepared in Hepes ph7.3 1M)/1X Phosphatase Solution/. 50X Phosphatase solution is prepared with 125 mM of NaF, 12.5 mM of NaVo4, 12.5 mM $NaPyroPO_4$ and 12.5 mM Glycerol-P. After 5 minutes of incubation at 95°C to reduce the disulfide bonds, recombinant Trypsin 1mg/mL (Proteomic Grade, Roche) is added to a ratio 1:50 (v/v) and proteins are digested into peptides overnight at 37°C. Reduced cysteines are then alkylated by the addition of 500 mM of iodocedamide. After 5 minutes of centrifugation at 25000g, the supernatant is transferred to a new tube. The pellet is then resuspended into 50 mM HEPES, and centrifuged again for 5 minutes at 25000g. This supernatant is then combined with the supernatant of the first centrifugation, allowing the dilution of the SDS by a factor 2 - for better Trypsin activity. Peptide concentration is then measured , according to the manufacturer's instructions with a Pierce™ BCA Protein Assay Kit (Thermo Scientific). Trypsin was added in a 1:100 ratio according to the BCA reading to allow further protein digestion (4 hours at 37°C). After centrifugation for 15 minutes at 25000g, the supernatant is spun down through a 0.22 uM column for 1 minute at 3000 rpm.

Samples are then cleaned up via a Mixed-mode reverse-phase CationXchange (Oasis® MCX LP Extraction Kits) to remove SDS from the mixture, and then on C18column (Sep-Pak® Vac C18 cartridge) to desalt the peptides further, according to the instructions of the manufacturer. Peptides concentration is measured every step with a Pierce™ BCA Protein Assay Kit (Thermo Scientific).

iTRAQ labeling

Five hundred micrograms of each digested sample was treated with one of the 4-plex iTRAQ reagents (Applied Biosystems) in 70% isopropanol at pH 7.2 for 2 h at room temperature. Labeled samples were dried down in a vacuum concentrator, and 250 µL of water was added to each tube to dissolve the peptides. Samples tagged with four different iTRAQ reagents were pooled together (using 50 µg of each sample for a total of 200 µg). Samples were centrifuged at 16,100 xg for 15 minutes. Supernatant was collected and centrifuged through a 0.22-µM filter and was used for liquid chromatography/tandem mass spectrometry (LC-MS/MS) analysis. iTRAQ labeling efficiency was calculated by searching the MS/MS data specifying four possible iTRAQ modifications: 1) fully labeled; 2) N-terminus-labeled only; 3) lysine-labeled only; and 4) non-labeled. Using the above protocol we obtained higher than 95% iTRAQ labeling efficiency for all datasets. Each biological replicate was labeled with two separate iTRAQ tags, giving two technical replicates within run. Non-infected samples were labeled with iTRAQ reagents 114, 115 and infected samples were labeled with iTRAQ reagents 116, 117. The labeled peptides are combined and analyzed by liquid chromatography and mass spectrometry (LC/MS/MS) for identification and quantitation.

After iTRAQ labeling, the peptides were loaded onto the HPLC online separation system using 3 columns, 2 RP (reverse phase) and 1 SCX (strong cation exchange). The first RP column is mainly used for sample loading and desalting. After washing, peptides are eluted to the SCX column using 0-80% ACN gradient. Then peptides are fractionated using increasing salt gradients. Spectra were acquired on LTQ linear ion trap tandem mass spectrometers. Signals of the iTRAQ reporter ions are used to calculate relative abundance of the peptides identified by the spectrum.

REFERENCES

Barr DJS (1980) An outline for the reclassification of the Chytridiales, and for a new order, the Spizellomycetales. Canadian Journal of Botany **58**: 2380–2394

Barr DJS (2001) Chytridiomycota, A Comprehensive Treatise on Fungi as Experimental Systems for Basic and Applied Research. *In* DJ McLaughlin, EG McLaughlin, PA Lemke, eds, Systematics and Evolution, The Mycota Volume 7A. Springer Berlin Heidelberg, Berlin, Heidelberg, pp 93–112

Bonardi V, Dangl JL (2012) How complex are intracellular immune receptor signaling complexes? Frontiers in plant science **3**: 237

Borowitzka MA, Moheimani NR (2010) Sustainable biofuels from algae. Mitigation and Adaptation Strategies for Global Change **18**: 13–25

La Camera S, Gouzerh G, Dhondt S, Hoffmann L, Fritig B, Legrand M, Heitz T (2004) Metabolic reprogramming in plant innate immunity: the contributions of phenylpropanoid and oxylipin pathways. Immunological reviews **198**: 267–84

Chisholm ST, Coaker G, Day B, Staskawicz BJ (2006) Host-microbe interactions: shaping the evolution of the plant immune response. Cell **124**: 803–14

Chisti Y (2007) Biodiesel from microalgae. Biotechnology advances **25**: 294–306

Consonni C, Bednarek P, Humphry M, Francocci F, Ferrari S, Harzen A, Ver Loren van Themaat E, Panstruga R (2010) Tryptophan-derived metabolites are required for antifungal defense in the Arabidopsis mlo2 mutant. Plant physiology **152**: 1544–61

Dangl JL, Jones JDG (2001) Plant pathogens and integrated defence responses to infection. Nature 411:

Denancé N, Sánchez-Vallet A, Goffner D, Molina A (2013) Disease resistance or growth: the role of plant hormones in balancing immune responses and fitness costs. Frontiers in plant science **4**: 155

Van Donk E, Ianora A, Vos M (2010) Induced defences in marine and freshwater phytoplankton: a review. Hydrobiologia **668**: 3–19

El-Sheekh MM, Khairy HM, El-Shenody R (2012) Algal production of extra and intra-cellular polysaccharides as an adaptive response to the toxin crude extract of Microcystis aeruginosa. Iranian journal of environmental health science & engineering **9**: 10

Engelberth J, Schmelz E a, Alborn HT, Cardoza YJ, Huang J, Tumlinson JH (2003) Simultaneous quantification of jasmonic acid and salicylic acid in plants by vapor-phase extraction and gas chromatography-chemical ionization-mass spectrometry. Analytical biochemistry **312**: 242–50

Freeman KR, Martin a P, Karki D, Lynch RC, Mitter MS, Meyer a F, Longcore JE, Simmons DR, Schmidt SK (2009) Evidence that chytrids dominate fungal communities in high-elevation soils. Proceedings of the National Academy of Sciences of the United States of America **106**: 18315–20

Ge P, Hao P, Cao M, Guo G, Lv D, Li X, Yan X, Xiao J, Yan Y, Agriculture S, et al (2013) iTRAQ-based quantitative proteomic analysis reveals new metabolic pathways of wheat seedling growth under hydrogen peroxide stress. Proteomics 1–36

Georgianna DR, Mayfield SP (2012) Exploiting diversity and synthetic biology for the production of algal biofuels. Nature **488**: 329–35

Gerphagnon M, Latour D, Colombet J, Sime-Ngando T (2013) A double staining method using SYTOX green and calcofluor white for studying fungal parasites of phytoplankton. Applied and environmental microbiology **79**: 3943–51

Glazebrook J (2005) Contrasting mechanisms of defense against biotrophic and necrotrophic pathogens. Annual review of phytopathology **43**: 205–27

Guschina IA, Harwood JL (2006) Lipids and lipid metabolism in eukaryotic algae. Progress in lipid research **45**: 160–86

Harwood A, Coates JC (2004) A prehistory of cell adhesion. Current opinion in cell biology **16**: 470–6

Hoffman Y, Aflalo C, Zarka A, Gutman J, James TY, Boussiba S (2008) Isolation and characterization of a novel chytrid species (phylum Blastocladiomycota), parasitic on the green alga Haematococcus. Mycological research **112**: 70–81

Huber O, Sumper M (1994) Algal-CAMs: Isoforms of a cell adhesion molecule in embryos of hte alga Volvox with homology to Drosohpila fasciclin I. The EMBO journal **13**: 4212–4222

Ibelings BW, De Bruin A, Kagami M, Rijkeboer M, Brehm M, Donk E Van (2004) Host Parasite Interactions Between Freshwater Phytoplankton and Chytrid Fungi (Chytridiomycota). Journal of Phycology **40**: 437–453

Jena J, Nayak M, Sekhar Panda H, Pradhan N, Sarika C, Ku. Panda P, V. S. K Rao B, B. N. Prasad R, Behari Sukla L (2012) Microalgae of Odisha Coast as a Potential Source for Biodiesel Production. World Environment **2**: 12–17

Jones CS, Mayfield SP (2012) Algae biofuels: versatility for the future of bioenergy. Current opinion in biotechnology **23**: 346–51

Kagami M, Bruin A, Ibelings BW, Donk E (2007) Parasitic chytrids: their effects on phytoplankton communities and food-web dynamics. Hydrobiologia **578**: 113–129

Kendrick B The Fifth Kingdom, 3rd ed. 1992

Langfelder P, Horvath S (2008) WGCNA: an R package for weighted correlation network analysis. BMC bioinformatics **9**: 559

Lawton K a, Friedrich L, Hunt M, Weymann K, Delaney T, Kessmann H, Staub T, Ryals J (1996) Benzothiadiazole induces disease resistance in Arabidopsis by activation of the systemic acquired resistance signal transduction pathway. The Plant journal : for cell and molecular biology **10**: 71–82

Letcher PM (2013) TEM Investigation of FD61 (putatively Paraphysoderma sedebokerense, Blastocladiomycota), an epibiotic parasite of Scenedesmus dimorphus. 61:

Letcher PM, Lopez S, Schmieder R, Lee PA, Behnke C, Powell MJ, McBride RC (2013) Characterization of Amoeboaphelidium protococcarum, an algal parasite new to the cryptomycota isolated from an outdoor algal pond used for the production of biofuel. PloS one **8**: e56232

Li X, Hu H, Zhang Y (2011) Growth and lipid accumulation properties of a freshwater microalga Scenedesmus sp. under different cultivation temperature. Bioresource technology **102**: 3098–102

Luo Y, Ahmed I, Kubátová A, Šťávová J, Aulich T, Sadrameli SM, Seames WS (2010) The thermal cracking of soybean/canola oils and their methyl esters. Fuel Processing Technology **91**: 613–617

Maeda H, Dudareva N (2012) The shikimate pathway and aromatic amino Acid biosynthesis in plants. Annual review of plant biology **63**: 73–105

Makarevi V, Andrulevi V, Skorupskait V (2011) Cultivation of Microalgae Chlorella sp . and Scenedesmus sp . as a Potentional Biofuel Feedstock. Environmental Research, Engineering and Management **3**: 21–27

Mandal S, Mallick N (2009) Microalga Scenedesmus obliquus as a potential source for biodiesel production. Applied microbiology and biotechnology **84**: 281–91

Margulis L, Chapman MJ (2009) Chytridiomycota. Kingdoms and Domains: An Illustrated Guide to the Phyla of Life on Earth. pp 217–219

Naoumkina MA, Zhao Q, Gallego-giraldo L, Dai X, Zhao PX, Dixon RA (2010) Genome-wide analysis of phenylpropanoid defence pathways. **11**: 829–846

Nichols D, Pessier A, Longcore J (1998) No Title. AAZV and AAWV Joint Conference. pp 267–271

Pieterse CMJ, Van der Does D, Zamioudis C, Leon-Reyes A, Van Wees SCM (2012) Hormonal modulation of plant immunity. Annual review of cell and developmental biology **28**: 489–521

Piotrowski JS, Annis SL, Longcore JE (2004) Physiology of Batrachochytrium dendrobatidis, a chytrid pathogen of amphibians. Mycologia **96**: 9–15

Potin P, Bouarab K, Salaün J-P, Pohnert G, Kloareg B (2002) Biotic interactions of marine algae. Current Opinion in Plant Biology **5**: 308–317

Prabakaran P, Ravindran AD (2012) Scenedesmus as a potential source of biodiesel among selected microalgae. Current Science **102**: 616–620

Radakovits R, Jinkerson RE, Darzins A, Posewitz MC (2010) Genetic engineering of algae for enhanced biofuel production. Eukaryotic cell **9**: 486–501

Rodolfi L, Chini Zittelli G, Bassi N, Padovani G, Biondi N, Bonini G, Tredici MR (2009) Microalgae for oil: strain selection, induction of lipid synthesis and outdoor mass cultivation in a low-cost photobioreactor. Biotechnology and bioengineering **102**: 100–12

Sparrow FK (1960) Aquatic Phycomycetes, 2nd ed. Michigan Press, Ann Arbor

Stephens E, Ross IL, Mussgnug JH, Wagner LD, Borowitzka M a, Posten C, Kruse O, Hankamer B (2010) Future prospects of microalgal biofuel production systems. Trends in plant science **15**: 554–64

Thaler JS, Humphrey PT, Whiteman NK (2012) Evolution of jasmonate and salicylate signal crosstalk. Trends in plant science **17**: 260–70

Thimm O, Bläsing O, Gibon Y, Nagel A, Meyer S, Krüger P, Selbig J, Müller L a., Rhee SY, Stitt M (2004) Mapman: a User-Driven Tool To Display Genomics Data

Sets Onto Diagrams of Metabolic Pathways and Other Biological Processes. The Plant Journal **37**: 914–939

Tran M, Van C, Barrera DJ, Pettersson PL, Peinado CD, Bui J, Mayfield SP (2013) Production of unique immunotoxin cancer therapeutics in algal chloroplasts. Proceedings of the National Academy of Sciences of the United States of America **110**: E15–22

Vélez CG, Letcher PM, Schultz S, Powell MJ, Churchill PF (2011) Molecular phylogenetic and zoospore ultrastructural analyses of Chytridium olla establish the limits of a monophyletic Chytridiales. Mycologia **103**: 118–30

Venteris ER, Skaggs RL, Coleman AM, Wigmosta MS (2013) A GIS cost model to assess the availability of freshwater, seawater, and saline groundwater for algal biofuel production in the United States. Environmental science & technology **47**: 4840–9

Wheeler GL, Miranda-Saavedra D, Barton GJ (2008) Genome analysis of the unicellular green alga Chlamydomonas reinhardtii Indicates an ancient evolutionary origin for key pattern recognition and cell-signaling protein families. Genetics **179**: 193–7